S. BARANNIKOVA, YU. LI

ISSN 0543-5846
METABK 60(1-2) 59-62 (2021)
UDC – UDK 669.1/669.14.15:539.374:620.172:620.16=111

KINETICS OF DEFORMATION BANDS IN A LOW-CARBON STEEL — STAINLESS STEEL BIMETAL

Received – Primljeno: 2020-06-25
Accepted – Prihvaćeno: 2020-10-25
Original Scientific Paper – Izvorni znanstveni rad

The regularities of non-uniform plastic deformation evolving on the Lüders bands are studied in a low carbon steel – austenite stainless steel bimetal via a digital image speckle method. The local strain distributions in the bimetal low-carbon steel base layer at the yield point stage are presented by the two strain localization bands that are similar to the Lüders bands. Analogous distributions arise at the yield point from the bimetal austenite stainless steel clad layer in the form of two strain localization fronts that are identical to the Portevin-Le Chatelier bands. Finally, the generation of strain localization bands is described in the context of a solid-state wedging model.

Key words: plasticity, deformation, localization, bimetal, Lüders bands, Portevin-Le Chatelier bands

INTRODUCTION

Macroscopic non-uniformity and instability of plastic flow arise at sample size scales as mutually consistent changes in stress-strain curves σ(ε) and strain localization patterns [1]. According to Refs. [2-5], plastic strain localization in metal alloys under stretching is manifested by the Lüders bands (LB) at the yield point stage or by the Portevin-Le Chatelier (PLC) effects at the discontinuous flow stages [6]. The main results on the kinetics of Lüders bands (LB) and PLC bands reveal both similarities and differences between these phenomena [5]. As for the similarity, it is worth mentioning that the LB fronts and the PLC bands are the macroscopic phenomena of plastic strain localization, which are the narrow moving bands with plastic strain inside them. Furthermore, both processes possess the same kinetics of generation, when plastic strain nuclei originate at the side surface of the working part of the sample and then germinate through the entire cross-section. Noticeable differences between these phenomena are observed at the developed strain localization stage associated with LB and PLC effects [5].

The study of the above mentioned processes consists in the analysis of the combined behavior of the LB and PLC fronts in a low carbon steel – austenite stainless steel bimetal system under loading. The known models of strength physics and failure mechanics, used for the description of deformation and demolition of monolithic materials and components of layered systems [7], do not allow one to assess plastic strain localization and failure in the layer connection zone. Thus this work is aimed at investigating the macroscopic plastic strain localization under uniaxial tension of a low carbon steel – austenite stainless steel bimetal system.

S. Barannikova, Yu. Li (e-mail: jul2207@mail.ru), Institute of Strength Physics and Materials Science of Siberian Branch Russian Academy of Sciences (ISPMS SB RAS), Tomsk, Russia; National Research Tomsk State University, Tomsk, Russia.

EXPERIMENTAL

Plastic strain localization of a bimetal at the yield plateau

A carbon steel - stainless steel bimetal was used as a sample. The base layer was ~ 6,7 mm thick and was composed of a low-carbon steel (See Table 1).

The thicknesses of the upper and bottom clad layers of the austenite stainless steel (See Table).) were ~ 0,75 mm. The bimetal sheet was produced by hot rolling of steel sheets at temperatures of 1 200 – 1 400 °C using a three-layer workpiece obtained by pouring liquid metal (low carbon steel) between the two clad sheets of stainless steel set in the mold. Such a bimetal can be considered as a model material for investigating the generation and propagation of strain at the interface of bcc and

Table 1 **Chemical composition of carbon steel (1) and – austenite stainless steel / wt. %**

Element	Steel (1)	Steel (2)
C	0,22	0,12
Si	0,3	0,8
Mn	0,65	2
Ni	0,3	9
P	0,04	0,035
Cr	0,3	19
N	0,008	-
S	0,05	0,02
Cu	0,3	0,3
As	0,08	-
Ti	-	1
Fe	rest	rest

FCC metals. As-prepared double shoulder samples with working part dimensions of 42 × 8 × 2 mm were stretched at 300 K at a rate of 6,67 × 10^{-5} s^{-1} using a LFM - 125 testing machine. The evolution of macroscopic strain localization bands was visualized at the different stages of strain hardening via a digital image speckle correlation method (DICSP) [8, 9]. For this, the sample under stretching was illuminated by a coherent semiconductor laser beam with a wavelength of 635 nm and a power of 15 w. The relevant images with superposed speckle patterns were recorded by a pixellink pl - b781 digital video camera at a frequency of 10 hz, digitated and saved as files.

The stress-strain curves $\sigma(\varepsilon)$ of bimetals consist of elastic strain, plastic strain and demolition ranges [10, 11].

The yield strength of the bimetal can be calculated using the rule of mixture for composites [12]:

$$\sigma_T^{(calc)} = \sigma_T^{(2)} \cdot (1-\alpha) + \sigma_T^{(1)} \cdot \alpha, \qquad (1)$$

where $\sigma_T^{(1)}$ and $\sigma_T^{(2)}$ are the yield strengths of the 1st and 2nd bimetal components; α is the fraction of the 1st component in the cross-section. In this case the fraction of the 1st component austenite stainless steel in the bimetal was 0,19 and was found as a ratio of the cross-section area of the component to the total cross-section area of the bimetal. The fraction of the 2nd component (low – carbon steel) in the bimetal achieved a value of 0.81; the yield strengths of the 1st and 2nd components were equal to 247 and 262 MPa. The yield strength of the bimetal, evaluated from Eq. (1), was 260 MPa, and the deviation from the relevant experimental value was ~ 4%.

The microstructure and the element composition of the bimetal in the connection zone were considered in detail in work [11]. The yield point in the bimetal stainless steel clad layer is followed by the emergence of microcracks with lengths $l \approx 5 \pm 1$ μm and a martensite α'-phase as a result of the γ - α' phase transition [13]. The amount of deformation α' – martensite in a stretched bimetal stainless steel clad layer was evaluated via X - ray diffraction (XRD). The X - ray diffractograms were acquired using the monochromatic CuKα radiation. According to the XRD analysis, the bimetal stainless steel surface layer in the initial state contains only austenite (γ - phase) with a lattice parameter a = 3,5999 Å. The bimetal samples exposed to tensile strain exhibit the strain-induced γ - α' phase transformation in the stainless steel surface layers [14] and a biphase structure with different ratios of α- and γ - phases. At the total strain ε_{tot} = 15 %, the α' - martensite content (a = 2.8873 Å) was found to be ≈ 52 ± 4 % and the rest was austenite (γ-phase) with a lattice parameter a = 3,5999 Å. Austenite stainless steel possesses a strain – unstable structure that may undergo the forced phase transitions with the formation of α' - phase particles [13]. The PLC features with varying temperature and tensile strain rate in the metastable austenite steel under stretching were thoroughly studied in work [13].

It is worth mentioning that the degree of strain of steel components is generally different from plastic strain of a three - layer low - carbon steel - austenite stainless steel –low - carbon steel material. Loading the bimetal composed of metals with various mechanical properties may give rise to additional internal stresses. In this respect, unlike the stainless steel, where the strain-induced γ - α' - phase transition occurs under severe plastic deformations [13], the martensite transformation in the bimetal stainless steel clad layer begins immediately after the end of the yield point. These structural modifications are expected to impact the local strain distributions upon loading.

Let us now consider the generation and propagation of the LBs at the yield point of the bimetal via the real - time digital image speckle correlation (DICSP) method [8, 9]. The emergence of a single local elongation center ε_{xx} was observed in the base layer of the material (low – carbon steel) at the total strain ε_{tot} = 0,006, whereas no localization centers ε_{xx} were detected in the austenite stainless steel clad layer (Figure 1a).

This means that macroscopic plastic strain localization in the form of CLBs generates at the beginning of plastic flow only in the bimetal base layer that undergoes strain prior to the clad layer. At the total strain ε_{tot} = 0,007 a single local elongation maximum ε_{xx}, corresponding to a plastic strain localization front, arises also in a thin stainless steel clad layer, whereas the LB nuclei of the base layer germinate along the sample width and achieve the bimetal compound boundary. At this moment, the LB fronts of the clad and base layers become to move as a whole toward the mobile clutch of the testing machine (Figure 1). Therefore the analysis of local strain distribution patterns reveals the emergence of a single LB front at the earlier stages of plastic flow, which propagates at the interface in the low-carbon base steel layer of a triple low - carbon steel - austenite stainless steel –low - carbon steel material.

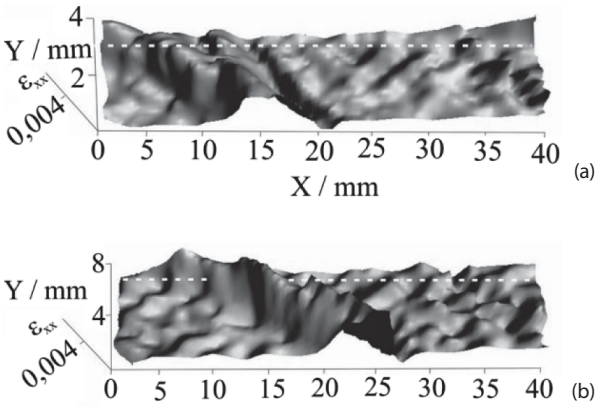

Figure 1 Generation and propagation of LBs in the base and clad layers of bimetal at the total strain: a) ε_{tot} = 0,0074; b) ε_{tot} = 0,009. The dotted line shows to the bimetal interface

This LB front then initiates the generation of the LB front in the stainless steel clad layer. For a system with-

out LBs at the beginning of the plastic deformation stage, the single localization front arising at the yield point stage spreads in both the base and clad layers (Figure 2). By analogy with PLC bands, the single plastic strain localization fronts for a monolithic stainless steel sample were observed under severe deformations at the discontinuous flow stage. They were caused by the interactions between the intercalated carbon atoms and the mobile dislocations in the martensite α' - phase formed by the strain-induced γ - α' phase transition [13]. The LBs in the clad layer are also likely due to α' -martensite detected in the bimetal surface layer at the end of the yield point stage.

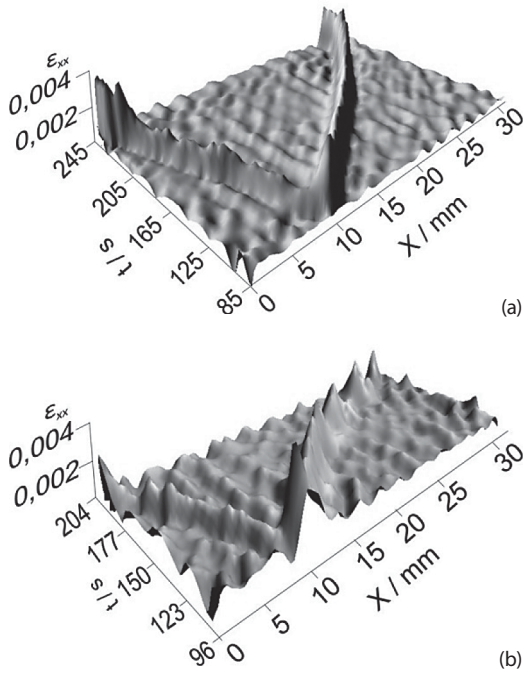

Figure 2 Propagation of LBs in bimetal at the yield point stage: a) low – carbon steel as a base layer; b) stainless steel as a clad layer

In a bimetal under loading, composed of metals with various mechanical properties the plastic flow originates in the soft metal base layer, whereas the firmer stainless steel clad layer undergoes more elastic deformation. Then both (base and clad) layers undertake the plastic strain at the yield point.

Two PLC fronts propagate oppositely in the upper stainless steel clad layer with velocities $V_1 = 0{,}7 \cdot 10^{-4}$ m/s and $V_2 = 2{,}3 \cdot 10^{-4}$ m/s (Figure 2b). Similar fronts are also observed in the lower stainless steel clad layer, which move oppositely with velocities $V_1 = 0{,}7 \cdot 10^{-4}$ m/s and $V_2 = 2{,}2 \cdot 10^{-4}$ m/s (Figure 2b).

The average velocity of propagation at the yield point of the bimetal low – carbon steel base layer is $V = 1{,}35 \cdot 10^{-4}$ m/s and that in the monolithic low-carbon steel is $V = 0{,}85 \cdot 10^{-4}$ m/s. Such average velocity at the yield points in the stainless steel clad layer is $V = 1{,}4 \cdot 10^{-4}$ m/s and that at the linear strain hardening in a monolithic stainless steel is $V = 0{,}15 \cdot 10^{-4}$ m/s.

Therefore one can affirm that the 750 μm thick stainless steel clad layer in case of bimetal does not suppress the formation of LBs, but increases the propagation velocity of the LB front in both the low – carbon steel base layer and the clad layer, as compared to data from the individual low – carbon and stainless steel components.

RESULT AND DISCUSSION

As seen in Figure 1, a single LB front in the bimetal first arises at the interface in the low – carbon steel base layer and then germinates across the sample width and achieves the opposite bimetal interface, which is typical of low – carbon steels at the yield points. No single strain localization fronts were observed in the room – temperature austenite stainless steels at the beginning of the plastic flow stage.

In order to understand the mechanism of PLC band formation in the bimetal stainless steel clad layer, let us use the wedging model proposed by Barenblatt [14]. Wedging is the process by which cracks in a solid body are formed by driving a hard wedge into it. During delamination, the adhesion forces acting between the opposite sides of the material to be torn are overcome gradually, and the crack faces close, forming a smooth profile similar to the picture when two pieces of glued material are torn off from each other [14]. The smooth closing of crack faces and limb stresses is the condition that allows one to evaluate the equilibrium crack, when wedging a solid [14]:

$$l = \frac{E^2 \cdot h^2}{4(1-\mu^2)^2 \cdot K^2} \qquad (2)$$

Here E is the Young's modulus, h – is the wedge width, μ – is the Poisson coefficient, and K – is the adhesion force characterizing the interaction of crack edges (the constant of the material). On the one hand, adhesion forces are effective in only the small vicinity of the crack end. On another, the surface density of forces within the area of their action is several orders of magnitude higher than the stresses induced in this area by external loads without the crack [14].

Applying the wedging model in regard to the PLC bands that are generated in the clad layer at the yield point stage, let us consider a LB as a wedge in the low – carbon steel base layer (Figure 3). Substituting the values $E = 2 \cdot 10^5$ MPa; $h = 10^{-4}$ m as a LB front width

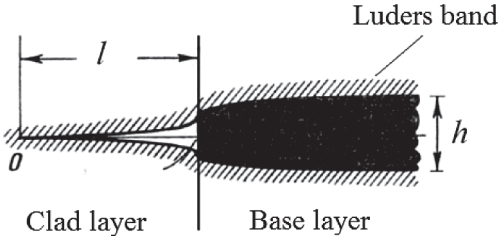

Figure 3 LB as the wedge element in the bimetal wedging model

in the base layer: μ = 0,3 – as the Poisson coefficient and K = 2,5 · 10^3 MPa · $M^{1/2}$ as the adhesion force for carbon steel [14] in Eq. (2), we obtain the length l ≈ 20 μm of a crack formed behind the wedge in the clad layer. As afore-mentioned, a microcrack with a length $l \approx 5 \pm 1$ μm was detected microscopically in the bimetal stainless steel clad layer. Hence one can affirm that the wedging force of the LB front in the base layer produces a microcrack as large as several microns, which makes local stresses concentrate in the clad layer.

Therefore it was shown that the LB arisen at the yield point of the bimetal low - carbon steel base layer may play role of a wedge in the Barenblatt wedging model, initiating the generation of the crack in the clad layer. Due to the high level of local stress at the interface, this LB favors the formation of the martensite α'-phase at the yield point. This leads to the emergence of PLC fronts in the stainless steel clad layer, which are detected during the discontinuous flow stage in monolithic stainless steels under severe plastic deformation.

CONCLUSION

- The LB arisen initially in the low-carbon steel clad layer at the stress equal to the yield strength at the yield point of the bimetal was found to initiate the crack formation in the stainless steel clad layer and to induce the emergence of a martensite α'-phase owing to a high level of local stresses at the interface. Furthermore, it gave rise to the PLC front in the stainless steel clad layer, which was detected at the discontinuous flow stage in monolithic stainless steels under severe deformations.
- A 750 μm thick stainless steel clad layer in deformed bimetal does not suppress the LB formation. Furthermore, it increases the propagation velocities of the LB fronts in the low-carbon steel base layer and in the clad layer in comparison with relevant values for the individual steel components.

Acknowledgments

This work was supported in the framework of the Program of fundamental scientific research of Russian State Academies of Sciences for 2013 – 2020, direction III.23.1.2 and the Program of competitiveness of National Research Tomsk State University.

REFERENCES

[1] L. B. Zuev, S. A. Barannikova. Autowave physics of material plasticity. Crystals 9 (2019), 458 - 487.
[2] M. A. Lebyodkin, D. A. Zhemchuzhnikova, T. A. Lebedkina, E. C. Aifantis, Kinematics of formation and cessation of type B deformation bands during the Portevin-Le Chatelier effect in an AlMg alloy. Results in Physics 12 (2019), 867-869.
[3] B. Mao, Y. Liao. Modeling of Lüders elongation and work hardening behaviors of ferrite-pearlite dual phase steels under tension. Mechanics of Materials 129 (2019), 222-229.
[4] A. A. Shibkov, M. F. Gasanov, M. A. Zheltov, A. E. Zolotov, V. I. Ivolgin. Intermittent plasticity associated with the spatio-temporal dynamics of deformation bands during creep tests in an AlMg polycrystal. International Journal of Plasticity 8 (2016), 37-55.
[5] L. B. Zuev. Chernov–Luders and Portevin–Le Chatelier deformations in active deformable media of different nature. Journal of Applied Mechanics and Technical Physics 58 (2017), 328-334.
[6] Pelleg J. Mechanical Properties of Materials. Dordrecht.: Springer, 2013. 634p.
[7] H. Li, L. Zhang, B. Zhang, Q. Zhang. Interfacial fracture behavior of a stainless/carbon steel bimetal plate in a uniaxial tension test. Results in Physics 14 (2019), 102470-1 - 102470-8.
[8] L. B. Zuev, V. V. Gorbatenko, K. V. Pavlichev. Elaboration of speckle photography techniques for plastic flow analyses. Measurement Science and Technology 21 (2010), 054014-1 - 054014-4.
[9] A. Kumar, A. Dutta, S. K. Makineni, M. Herbig, R. H. Petrov, J. Sietsma. In-situ observation of strain partitioning and damage development in continuously cooled carbide-free bainitic steels using micro digital image correlation. Materials Science and Engineering: A 757 (2019), 107-116.
[10] S. Barannikova, Y. Li, L. Zuev. Research of the plastic deformation localization of bimetal. Metalurgija 57 (2018), 275-278.
[11] S. Barannikova, L. Zuev, Y. Li. Plastic flow heterogeneity and failure of bimetal material. International Journal of GEOMATE 14 (2018), 112-117.
[12] A. K. Kaw. Mechanics of composite materials, 2nd ed., Boca Raton: CRC Press, Taylor & Francis Group (2006), 457.
[13] A. Müller, C. Segel, M. Linderov, A. Vinogradov, A. Weidner, H. Biermann. The Portevin–Le Châtelier Effect in a Metastable Austenitic Stainless Steel. Metallurgical and Materials Transactions A: Physical Metallurgy and Materials Science 47 (2016), 59-74.
[14] G. I. Barenblatt. Equilibrium cracks formed during brittle fracture rectilinear cracks in plane plates. Journal of Applied Mathematics and Mechanics 23 (1959), 1009-1029.

Note: The response for English language is YU.V Stankina the translation professional of National Research Tomsk State University «TSU»